Cross-scale spatial variability and associations of carbon pools provide insight into regulating carbon sequestration in tropical montane rainforests

Zhangqi Ding[1,2], Zhijian Mou[1,2,3], Yanpeng Li[4], Chao Liang[5], Zicai Xie[1,2,3], Jun Wang[1,2], Dafeng Hui[6], Hans Lambers[7], Jordi Sardans[8,9], Josep Peñuelas[8,9], Han Xu[4*], Zhanfeng Liu[1,2*]

[1] Key Laboratory of Vegetation Restoration and Management of Degraded Ecosystems & CAS Engineering Laboratory for Vegetation Ecosystem Restoration on Islands and Coastal Zones, South China Botanical Garden, Chinese Academy of Sciences, Guangzhou 510650, China

[2] South China National Botanical Garden, Guangzhou 510650, China

[3] College of Resources and Environment, University of Chinese Academy of Sciences, Beijing 100049, China

[4] Research Institute of Tropical Forestry, Chinese Academy of Forestry, Longdong, Guangzhou 510520, China

[5] Key Laboratory of Forest Ecology and Management, Institute of Applied Ecology, Chinese Academy of Sciences, Shenyang 110016, China

[6] Department of Biological Sciences, Tennessee State University, Nashville, TN 37209, USA

[7] School of Biological Sciences, University of Western Australia, Perth, WA 6009, Australia

[8] CSIC, Global Ecology Unit CREAF-CSIC-UAB, Cerdanyola del Valles, Catalonia 08193, Spain

[9] CREAF, Cerdanyola del Valles, Catalonia 08193, Spain

Correspondence:

Zhanfeng Liu, E-mail: liuzf@scbg.ac.cn; Han Xu, E-mail: hanxu81@gmail.com

Abstract

The spatial distribution of plant, soil, and microbial carbon pools, along with their intricate interactions, presents a great challenge for the current carbon cycle research. However, it is not clear what are the characteristics of the spatial variability of these carbon pools, particularly their cross-scale relationships. We investigated the crossscale spatial variability of microbial necromass carbon (MNC), soil organic carbon (SOC) and plant biomass (PB), as well as their correlation in a tropical montane rainforest using multifractal analysis. The results showed multifractal spatial variations of MNC, SOC, and PB, demonstrating their adherence to power-law scaling. MNC, especiallly low MNC, exhibited stronger spatial heterogeneity and weaker evenness compared with SOC and PB. The cross-scale correlation between MNC and SOC was stronger than their correlations at the measurement scale. Furthermore, the cross-scale spatial variability of MNC and SOC exhibited stronger and more stable correlations than those with PB. Additionally, this research suggests that when SOC and PB are both low, it is advisable for reforestations to potentiate MNC formation, whereas when both SOC and PB are high some thinning can be advisable to favour MNC formation. Thus, these results support the utilization of management measures such as reforestation or thinning as nature-based solutions to regulate carbon sequestration capacity of tropical forests by affecting the correlations among various carbon pools.

Keywords: Microbial necromass carbon, Spatial variability, Multifractal analysis, Joint multifractal analysis, Plant biomass, Soil organic carbon

1. Introduction

Soil organic carbon (SOC) is formed by the accumulation of carbon input from plants, invertebrates and microorganisms (Kögel-Knabner and Rumpel, 2018). As the largest terrestrial organic carbon pool (Eswaran et al., 1993), SOC plays an important role in the global carbon cycle (Lehmann and Kleber, 2015; Liang et al., 2019). Serving as the basic biological components of terrestrial ecosystems, microbes are closely associated with the dynamics of SOC via two pathways: catabolic mineralization to produce energy (and thus CO_2) or biomass (Prommer et al., 2020), and anabolic reactions (cell synthesis) and sequestration of their residues to form persistent carbon in soil (Miltner et al., 2012; Cotrufo et al., 2013). Although microbial biomass occupies a small proportion of SOC (< 5%), the production and continuous accumulation of soil microbial necromass carbon (MNC) during microbial metabolic activities contribute significantly to SOC accumulation (Liang et al., 2017). For example, comprehensive analyses by Liang et al. (2019) and Wang B. et al. (2021) found that MNC, on average, accounts for approximately 35% of SOC in forest ecosystems. Moreover, MNC has a relatively longer turnover time than its living carbon (biomass) and contributes more to the formation of SOC pools (Liang et al., 2011; Kuzyakov et al., 2014). Therefore, an in-depth exploration of MNC can advance our understanding of the composition and variation of SOC which is crucial for managing and predicting soil carbon pools in terrestrial ecosystems.

Amino sugars are an important component of microbial cell walls and are widely accepted as biomarkers of MNC due to their exclusive presence in microorganisms, rather than in plants which contributes to our understanding of microbial involvement in soil carbon cycling (Joergensen, 2018). In addition, the changes of different amino sugar compounds in the soil can help differentiate the accumulation of fungal- (FMNC) and bacterial-derived microbial necromass carbon (BMNC) and evaluate their contributions to SOC accumulation (Kimble et al., 2000; Joergensen, 2018). In general, fungal-derived glucosamine (GluN) can be calculated by subtracting bacterial-derived GluN from the total amount of GluN, as muramic acid (MurN) is exclusively present in bacterial cell walls while GluN is found in both fungal and bacterial cell walls. BMNC and FMNC were then obtained based on MurN and fungal-derived GluN (Mou et al., 2021). The concentration of FMNC in soil tends to be significantly higher than that in its bacterial counterpart (BMNC) due to the greater biomass of fungi (He et al., 2020) and the slower decomposition of fungal cells (Wang B. et al., 2021).

The accumulation of MNC depends on the balance between microbial biomass production and decomposition, two processes affected by various biotic and abiotic factors (Buckeridge et al., 2020).

Numerous studies have explored the relationship between biotic (Prommer et al., 2020) (such as diversity or biomass of plants and microorganisms), abiotic factors (Wang B. et al., 2021) (such as pH, nitrogen and phosphorus concentrations), and MNC (both FMNC and BMNC) (Khan et al., 2016; Buckeridge et al., 2022), but the spatial distribution patterns and potential driving mechanisms of MNC are still uncertain. There is a knowledge gap in the distribution patterns of MNC in terrestrial ecosystems, especially in tropical forest ecosystems, a hotspot in global carbon cycling research which stores more than half of global forest carbon through living (above- and belowground) biomass, litter, and soil (approximately 46 percent of the world's living terrestrial carbon or 11 percent of the world's soil carbon) (Bonan, 2008; Pan et al., 2011), and has the fastest SOC turnover (Sayer et al., 2019).

The spatial distribution and mechanism of soil MNC are mainly carried out based on transect or point sampling methods along elevation gradients at the local scale or across latitudinal gradients at the regional scale. For example, the altitudinal distribution of BMNC in a subtropical forest is unimodal due to the influence of soil moisture and nutrient availability (Mou et al., 2021). The latitudinal distribution of MNC/SOC is controlled by climatic and edaphic factors (Tian et al., 2022). Some studies have also revealed the vertical variation mechanism of MNC with soil depth in different ecotypes (agriculture, grassland, and forest) at the global scale (Ni et al., 2020; Wang B. et al., 2021). However, in general, other pattern characteristics (such as spatial autocorrelation or aggregation) that may exist in MNC are rarely explored and reported compared with microbial diversity (Song et al., 2018; Kärnä et al., 2019) or SOC (Tang et al., 2017; Wiesmeier et al., 2019). The “inherent spatial autocorrelation” resulting from the reproduction or spread of microorganisms and the “induced spatial dependency” caused by factors such as resource and energy inputs, as well as climate (Dale and Fortin, 2014), may crucial for revealing the spatial variation mechanism of MNC. In particular, the potential impact between adjacent plots is still unclear, such as whether soil particle size or plants in adjacent plots affect the MNC concentration of the specific quadrat. Knowledge on these aspects may greatly benefit the construction and accuracy of carbon-related models (Fan et al., 2021).

Compared with the sample points or transect lines established in short-term experiments, fixed-monitored grid-type plots with more detailed biotic and abiotic information were selected in this study. Through a comprehensive analysis of the spatial data of MNC (including FMNC and BMNC), topographic features, and soil and plant properties within the monitoring plot, we aimed to reveal: 1) the spatial distribution pattern of soil MNC and MNC/SOC in tropical rainforests; 2) the mechanism of effects of topographic features, and soil and plant properties on soil MNC.

2. Materials and methods

2.1 Study site

This study was conducted at the Jianfengling (JFL) 60-ha tropical montane rainforest site (1000 m × 600 m), located in the Ledong Li Autonomous County of Hainan province, China (18.7308°N, 108.9050°E) (Fig. 1). The elevation of the study site varies from 866 m to 1017 m. The study site has a tropical monsoon climate with a mean annual precipitation of 2449 mm, and the mean annual air temperature is 19.8°C. The 60-ha site was established in 2011 and the first and second plant censuses were completed in 2012 and 2019, respectively. The top five dominant plant species in this study site are *Livistona saribus*, *Gironniera subaequalis*, *Cryptocarya chinensis*, *Alseodaphne hainanensis* and *Prismatomeris tetrandra*. More detailed information about the study site can be found at https://forestgeo.si.edu/sites/asia/hainan.

2.2 Sample collection and processing

The 60-ha study site was divided into 500 subplots (40 m × 30 m). The surface soil (0-10 cm) within 12 quadrats (10 m × 10 m) in each subplot was collected by soil cores and mixed into one sample. Thus, a total of 500 representative soil samples were obtained in 2013. After sieving to 2 mm to remove stones, roots or other impurities, all soil samples were air-dried at room temperature and further ground for the analysis of amino sugars and other physicochemical properties. Soil bulk density was determined by the core ring method (Al-Shammary et al., 2018). Soil water content was determined gravimetrically by weighing soil after drying in an oven at 105°C for 48 h. Soil texture was determined by the hydrometer method (Malvern Panalytical, Malvern, UK). The concentrations of SOC and total nitrogen (TN) were measured with the Flash 2000 HT elemental analyser (Thermo Fisher Scientific, Waltham, USA). Soil total phosphorus (TP) and plant-available phosphorus (AP) concentration were analysed by molybdenum antimony colorimetry with a UV spectrophotometer after H_2SO_4-$HClO_4$ digestion (Khan et al., 2016) and NH_4F-HCl extraction respectively. Soil pH was measured using the soil slurry method with a glass electrode, where the ratio of deionized water volume to soil mass was 2.5:1.

Microbial necromass carbon concentration was estimated based on three amino sugars (glucosamine, GluN; galactosamine, GalN; and muramic acid, MurN):

FMNC (mg kg^{-1} dry soil) = (total GluN - 2 × MurN × 179.2 / 251.2) × 9

BMNC (mg kg^{-1} dry soil) = MurN × 45

In this study, MNC is the sum of FMNC and BMNC. Since GluN is found in both fungal and bacterial

cell walls, the quantification of fungal-derived GluN is achieved by deducting the bacterial-derived GluN from the total GluN. Detailed theories and calculation formulas can be found in Liang et al. (2019). Among them, soil amino sugars were extracted and determined according to the method of Indorf et al. (2011). The identification and quantification of GluN, GalN, and MurN were performed by a Dionex RS 3400 fluorescence detector (high-performance liquid chromatography, Dionex Ultimate 3000, Thermo Fisher Scientific, Waltham, USA). Specific measurement steps can be found in Mou et al. (2021).

Then, the topographic features of the study site were calculated. According to the original elevation information of the study site on the 20 m × 20 m scale, the elevation value of the four corners of each 40 m × 30 m subplot was calculated by ordinary Kriging interpolation, and then the average was taken as the elevation of this subplot. Convexity was the elevation difference between the subplot of interest and the eight subplots around it. The slope was the maximum rate of change in value from that subplot to its eight neighbours, while the aspect identifies the downslope direction of the maximum rate of change in value from each subplot to its eight neighbours (Burrough et al., 2015). Aspect is the slope direction. The original elevation information and raw vegetation data for each 20 m × 20 m subplot were obtained in the first plant censuses (Xu et al., 2015). The elevation, latitude, and longitude of the four corners of each 20 m × 20 m subplot were recorded using a global positioning system (GPS).

Similarly, the raw vegetation data from the study site was processed. Based on the 20 m × 20 m scale plant diversity (richness, abundance, and biomass), scale transformation was performed through interpolation to obtain 40 m × 30 m scale data corresponding to soil and topographic data. Here, we use the basal area to represent the biomass of the aboveground plant.

2.3 Statistical analyses

We first summarized the concentrations of soil microbial necromass carbon (MNC, FMNC, and BMNC) and their proportions in SOC (MNC/SOC, FMNC/SOC, and BMNC/SOC), and calculated the coefficients of variation (CV; standard deviation divided by the mean). Then, we used the Kolmogorov-Smirnov (K-S) test to verify whether their probability of appearing in each subplot conformed to a uniform distribution, thereby judging whether soil microbial necromass carbon concentrations and their proportions in SOC followed complete spatial randomness (CSR).

Moran's I test was used to identify the significant spatial autocorrelation association at the "global" and "local" scale based on the locations of 500 subplots (Bivand and Wong, 2018). The Moran's I statistic of global indicators of spatial association (GISA) ranges from -1 to +1. If $I = 0$, it means that the spatial

distribution is random; if I >0, it represents that the distribution has a positive autocorrelation, and vice versa. According to the statistical results of local Moran's I, spatial autocorrelation falls into four types. High-high clustering pattern means that the value is also higher in the neighbouring of the areas with high values. Low-low clustering pattern refers that the value of the neighbouring of the low value area is also low. High-low clustering pattern means that the value is lower in the neighbouring of the high value area. Low-high clustering pattern means that the value is higher in the neighbouring to the area with the low value. Local indicators of spatial association (LISA) based on first order neighbours using the "queen contiguity" selection rules were taken to identify and map the statistically significant spatial aggregation of soil MNC, FMNC, and BMNC concentrations, and their proportions in SOC (Anselin, 1995). Spatial correlation was calculated via global bivariate Moran's I (Wartenberg, 1985). The spatial weight list was determined as the inverse distance of neighbours. The spatial weight list involved in calculations such as Moran's I test and structural equation models (SEM) in this paper was identical.

Piecewise structural equation modelling (pSEM) has good compatibility with spatial autocorrelation, and can more flexibly adapt to the violation of normality and independence in regression model assumptions (Lefcheck, 2016). Here, we used pSEM to examine the direct and indirect effects of soil properties (pH, TN, TP, etc.), plant properties (richness, abundance, and biomass), and topographic features (elevation, convexity, slope, and aspect) on soil microbial necromass carbon (MNC, FMNC, and BMNC) concentrations and their proportions in SOC (MNC/SOC, FMNC/SOC, and BMNC/SOC). First, we used exploratory factor analysis (EFA) to extract common factors for topographic features, and soil and plant properties, respectively, and incorporated them into the SEM as latent variables to take into account their simplicity and accuracy. Then, we assumed that topographic features had direct impacts on soil and plant properties, and soil properties also had direct impacts on plant properties. We also calculated bivariate correlations to account for any potential covariance between factors unaccounted for by the topographic features or soil properties. Therefore, we tested whether topographic features can affect soil MNC, FMNC, and BMNC concentrations, and their proportions in SOC directly or indirectly through soil and plant properties. Considering the influence of spatial autocorrelation from adjacent plots, we chose the spatial simultaneous autoregressive model (SAR). There are three alternative SAR model specifications (the SAR-lag model, the SAR-error model, and the SAR-sac model), and which type was suitable for each of the component models within the pSEM was determined by the classical Lagrange Multiplier (LM) test (Elhorst, 2012) and their ecological implications. We also tested the multicollinearity between these latent variables

based on variance-inflation factors (VIF, all lower than 2.2). The goodness of fit of the SEM was evaluated following the recommendations of Lefcheck (2016).

Construction of neighbour lists, spatial weight calculation of neighbour lists, Moran's I test, bivariate Moran's I, and classical Lagrange multiplier tests, and SAR models were accompanied using the package "spdep" and "spatialreg"; structural equation modelling was done using the "piecewiseSEM" package. All data analyses were completed in R (R Core Team, 2021) (version 4.1.2).

3. Results

3.1 Concentrations of soil microbial necromass carbon

Soil MNC (9.5 ± 2.8 g kg^{-1}) was an important component of SOC in a tropical rainforest and the contribution of MNC to SOC was approximately 36% (range from 18% to 55%) (Fig. 2). In addition, FMNC was the dominant constituent of MNC with a concentration of 7.8 ± 2.2 g kg^{-1} and a 30 ± 6.2 percentage of SOC, approximately 4.7 times higher than its bacterial counterpart (1.7 ± 0.7 g kg^{-1} and 6.3 ± 1.9% of SOC, respectively) (Fig. 2). The spatial variation of soil MNC, FMNC, and BMNC concentrations, and their proportions in SOC were large (CV > 20%) (Fig. 2).

3.2 Spatial pattern of soil MNC and related environmental factors

The spatial distribution patterns of soil microbial necromass carbon concentrations and their proportions in SOC were different (Fig. 3), and the spatial correlation coefficients were all between 0.4 and 0.7 (Fig. A.1). The spatial distribution of FMNC and FMNC/SOC was more similar to MNC and MNC/SOC than BMNC and BMNC/SOC (0.69>0.66, and 0.62>0.56, Fig. A.1), respectively, given that MNC was mainly composed of FMNC (approximately 83% on average, range from 72% to 89%).

In addition, we also observed differences in the spatial distribution of soil pH, SOC, TN, TP, AP, and stoichiometric ratios (C:N, C:P, N:P) in the tropical rainforest soil (Fig. 4). The spatial variation of topographic features, such as elevation and slope as well as plant diversity and biomass were also different. Among them, except that the CV of pH and elevation was less than 5% and that of plant richness less than 10%, the CVs of other variables were all greater than 20% (that is, with greater variation). Detailed information on each environmental factor can be found in Appendix (Part-1).

The results of the K-S test indicated that both soil microbial necromass carbon concentrations and their proportions in SOC, and these environmental factors were not following a completely spatially random distribution. The global indicators of spatial association results showed that the distribution of soil MNC,

FMNC, and BMNC concentrations, and their proportions in SOC had significant spatial autocorrelation (Fig. 5). The local indicators of spatial association map also showed that the spatial distribution of soil microbial necromass carbon concentrations and their proportions in SOC both had significant high-high and low-low clustering patterns, but they were not identical. Similarly, the spatial autocorrelation patterns of FMNC and FMNC/SOC were similar to those of MNC and MNC/SOC, respectively.

3.3 Regulation of soil MNC by environmental factors

Structural equation model results showed that soil MNC, FMNC, and BMNC concentrations were directly related to topographic features (elevation and convexity) and soil properties (except C:N ratio and texture), whereas plant diversity and biomass had no significant effect on soil microbial necromass carbon accumulation (Appendix Part-2). Soil fertility parameters (C/P, N/P, SOC, TN, pH, TP, AP) played a stronger role than physical properties (texture and moisture content). Standardized direct effects are the path coefficients in the model, (e.g., from TOPO1 to MNC, 0.188, Fig. A.2). Indirect effects are all mediating effects. For example, changes in slope and aspect affect MNC, too. The indirect effect and is the product of the path coefficients (e.g., from TOPO2 to SPHY2, 0.144, Fig. A.2) and (from SPHY2 to MNC, 0.050, Fig. A.2). If there were other paths in the model such that MNC changed when TOPO2 changed, those effects would be added to the indirect effect as well. This study reports total indirect effects. The standardized total effect is the sum of the standardized direct and indirect effects. The standardized total effect of soil properties was greater than that of topographic features, and the direct effect of topographic features was greater than its indirect effect.

In contrast to the positive effects of environmental factors such as topographic features and soil properties on soil microbial necromass carbon concentration, the proportion of microbial necromass carbon in SOC (MNC/SOC, FMNC/SOC, and BMNC/SOC) was significantly directly or indirectly limited by topographic features, and soil and plant properties, but the total effect of soil properties was still the strongest (Fig. 6). Both soil properties (except SBD and SMC) and plant biomass were directly negatively correlated with MNC/SOC and FMNC/SOC. The effect of C:N ratio is much greater than that of other soil physicochemical properties, and topographic features or plant properties. Topographic features such as elevation and slope mainly played an indirect negative role by affecting soil properties or plant properties, although they were still directly and positively related to MNC/SOC and FMNC/SOC. BMNC/SOC was negatively correlated with soil chemical properties (especially C:N ratio, except TP and AP), and indirectly related to topographic features, while plant and soil physical properties had no significant effect on it.

Detailed structural equation model results of soil microbial necromass carbon concentrations and their proportion in SOC can be found in Appendix (Part-2). Among them, spatial simultaneous autoregressive model results also show that considering the spatial relationship significantly improved the fit of the regression model (drastic reduction in AIC), and more accurately revealed the mechanism of various environmental factors, whether it was for soil microbial necromass carbon concentrations or their proportion in SOC. The significance of rho (ρ) in the SAR model suggests that adjacent plots were very important in predicting specific quadrat values for MNC/SOC and FMNC/SOC. The significance of lambda (λ) also indicates that there were other factors not included that influenced the spatial variation of MNC, FMNC, BMNC, and BMNC/SOC. More detailed results of SAR can be found in Table A.2.

4. Discussion

Our results show that in the Jianfengling (JFL) rainforest, the soil MNC concentration was relatively low (7.8 ± 2.2 g kg^{-1} on average) compared with global temperate forests (approximately 32 g kg^{-1}, Liang et al., 2019) or forest ecosystems (approximately 17 g kg^{-1}, Wang B. et al., 2021), and the concentration of FMNC was significantly higher than that of BMNC which collectively accounted for 36% of the SOC, on average. The soil in tropical forest ecosystems has a high input from the net primary productivity (NPP) through dead wood, litter, and root exudates. However, a higher priming effect (Sayer et al., 2011), and slower decomposition of plant-derived SOC (such as lignin and cellulose) (Algora Gallardo et al., 2021; Wang B. et al., 2021), may have contributed to the lower levels of soil SOC and available carbon concentrations in this region (Chen et al., 2020; Liang et al., 2019). Higher mean annual temperature and sand proportion (up to 60% on average) affect the sorption and desorption of necromass carbon, reducing the protective effect of clay particles and accelerating its turnover (Buckeridge et al., 2022; Hu et al., 2020). Resulting in faster carbon turnover and lower levels of soil FMNC and BMNC concentrations in JFL than in temperate forests or grasslands, as summarized by Liang et al. (2019) and Wang B. et al. (2021). In forest ecosystems, the living fungal-bacterial biomass ratio (based on phospholipid fatty acid data) is often as high as four (He et al., 2020), and complex organic matter is mainly decomposed by fungi (Xia et al., 2020); fungal-derived necromass carbon is relatively stable in soil (e.g., residual chemistry and fungal morphology) (Adamczyk et al., 2019), which might account for the higher FMNC/BMNC ratio in the current study (approximately 4.7).

In this study, soil MNC, FMNC, and BMNC concentrations, and their proportions in SOC exhibited high spatial variability (CVs were all greater than 20%) in a tropical rainforest, and the spatial variation of

BMNC and BMNC/SOC was slightly larger than that of FMNC and FMNC/SOC, respectively. Compared with the common spatial distribution of microbial community (Meyer et al., 2018; Peng et al., 2019), soil MNC, FMNC, and BMNC concentrations showed stronger spatial autocorrelation. This may be due to the strong tolerance and adaptability (like dormancy) of microorganisms to fine-scale adverse environments, reducing the species' turnover and distance decay effects (Locey et al., 2020), thereby weakening the spatial autocorrelation of richness or diversity. However, local in situ resource conditions such as organic carbon and nitrogen may significantly alter microbial living carbon (biomass), leading to significant context-dependent spatial autocorrelation (Zhao et al., 2009), thus affecting the spatial distribution of MNC. In particular, the high-high and low-low clustering patterns of soil microbial necromass carbon concentrations and their proportions in SOC, reported for the first time here, indicates that concentrations estimated at the local scale based only on insufficient random arrangements sample lines or points may exhibit large biases. Soil microbial necromass carbon concentrations and their proportions in SOC may be overestimated by sampling patches with high concentrations but underestimated in low-concentration patches. Future research should not ignore such spatial pattern characteristics and sampling scales (grain). This significant spatial autocorrelation of the distribution of soil MNC, FMNC, and BMNC concentrations and their proportions in SOC can better reveal their responses to environmental variation in tropical forests, and may also improve the accuracy and application of current soil carbon models (Vasques et al., 2010).

We found that the mechanisms affecting the spatial variation of FMNC and BMNC were similar, although their distribution patterns were different. The elevation variation within the JFL study site was small (approximately 150 m, CV is 3%), while the spatial variability of soil and plant properties was very high (except pH and Richness). On the local scale, the soil microbial necromass carbon concentration change was mainly dominated by the spatial heterogeneity of soil properties, followed by topographic features, while plant properties had no significant effect on it. Soil moisture content could significantly promote the soil microbial necromass carbon accumulation, and sometimes indirectly modulate MNC or MNC/SOC by altering above- or belowground biodiversity or biomass (Yang et al., 2008; He et al., 2022). The results of Mou et al. (2021) in subtropical forests also show that soil nutrients may significantly be related to the spatial variation of FMNC and BMNC along an altitudinal gradient. In soils with high levels of nutrients, more microbial necromass carbon is continuously stabilized by the mineral matrix due to rapid turnover of microbial biomass (Müller et al., 2017), which promotes its accumulation in the soil (Liang et al., 2017). Moreover, the pH in this region was low (less than 5.5), and a slight change might trigger a dramatic change

312 in microbial carbon-use efficiency (Jones et al., 2019), thus significantly associated with the soil microbial
313 necromass carbon concentrations and their proportions in SOC. Lower pH may promote the FMNC/BMNC
314 ratio by increasing fungal biomass (Grosso et al., 2016). However, different from the results of Ni et al. (2020)
315 on the global scale, the C:N ratio had no significant effect on the change of MNC, as well as FMNC and
316 BMNC. This may be due to the low levels of SOC in this region, forming a community dominated by highly-
317 efficient nutrient-acquiring microorganisms (rather than high yield strategies) (Shao et al., 2021), thus
318 limiting the production and accumulation of microbial necromass carbon. In general, the effect of SOC, TN,
319 and pH on FMNC concentration variation was higher than that of TP and AP, but they were opposite in
320 BMNC concentration change. High P availability is probably more conducive to bacterial growth and
321 reproduction and may be a potential limiting nutrient for bacterial communities in JFL tropical rainforests.
322 Although both topographic features (elevation, convexity and aspect) and soil chemical properties (SOC,
323 total nitrogen, total phosphorus) were positively correlated with soil MNC, FMNC, and BMNC concentration,
324 they were negatively related to their proportion in SOC. Different from the results of Wang C. et al. (2021),
325 we found that clay content significantly related to MNC/SOC and FMNC/SOC, but not MNC and FMNC,
326 probably because it promoted faster accumulation of other components such as plant-derived SOC. Increased
327 N generally leads to a shift in the microbial community from fungal to bacterial dominance (Hu et al., 2022),
328 thus reducing the FMNC/SOC ratio (Zhang et al., 2016). Furthermore, SEMs showed that topographic
329 features (elevation and convexity) and soil properties (like pH and TN) significantly altered plant diversity
330 and biomass. We suggest that despite the abundant and richness input of root exudates or litter, the metabolic
331 and reproductive needs of fungi might still not be met due to the slow decomposition of plant-derived carbon.
332 Therefore, in this scenario the decomposition and utilization of FMNC by fungi would be promoted, slowing
333 down the accumulation of FMNC, increasing the relative accumulation difference between them (plant-
334 derived carbon and FMNC), and leading to the decrease of FMNC/SOC. Moreover, we found that the effects
335 of soil TP and AP and plant properties on BMNC/SOC were not significant. Given the low phosphorus
336 availability in this region (Mori et al., 2018), other components of SOC also increased with soil phosphorus
337 concentration (e.g., FMNC), resulting in less prominent changes in BMNC/SOC.
338 In this study, a large part of the spatial change of soil microbial necromass carbon concentrations and
339 their proportions in SOC in tropical rainforests were explained by 17 biotic and abiotic factors based on SAR
340 model results. Future research can be conducted considering the following aspects. First, the significance of
341 coefficient λ (lambda) in multivariate spatial regression models (Table A.2) indicates that factors that were

not included in this study, such as soil temperature, fungal and bacterial diversity or biomass, may also directly or indirectly be associated with spatial variation of soil MNC, FMNC, and BMNC concentrations, and their proportions in SOC. Second, given the large variation in the distribution of soil microbial necromass carbon and its obvious spatial aggregation characteristics, it is difficult to reveal the real distribution mechanism by point or line sampling at a single scale. We expect to verify and adjust soil carbon dynamics-related models in the future based on more spatial-temporal data or integrate the results of multi-scale and multi-ecosystem research. Third, isotope analysis can be applied to trace potential flow pathways and mechanisms of soil microbial necromass carbon and other derived SOC (Whalen et al., 2022; Yang et al., 2022), or particulate organic carbon and mineral-associated organic carbon. Soil microbial necromass carbon often has significant vertical depth variation (Wang B. et al., 2021), but its horizontal distribution at different depths and spatial scales are still not clear. Understanding the vertical distribution and mechanism may help us assess or predict soil carbon dynamics more accurately.

5. conclusions

In summary, both soil microbial necromass carbon concentrations and their proportions in SOC exhibited high spatial variability and significant high-high and low-low clustering patterns in a tropical rainforest at local scales, implying that low sampling resolution may lead to large uncertainties in estimating soil carbon dynamics at specific sites. Furthermore, we determined that the spatial variation of soil microbial necromass carbon concentrations was mainly positively correlated with soil chemical properties (such as SOC, total nitrogen, and total phosphorus) and topographic features (elevation, convexity, and aspect), whereas their proportions in SOC were just the opposite (especially the C:N ratio). MNC/SOC and FMNC/SOC were also significantly and negatively associated with aboveground plant biomass, although they did not relate to the spatial distribution of soil MNC and FMNC concentrations. The different variation between soil microbial necromass carbon accumulation and its contribution to SOC is possibly due to the faster accumulation of plant-derived organic carbon in this region. This study, for the first time, showed the spatial distribution pattern of soil microbial necromass carbon in a tropical rainforest and revealed the effects of topographic features, and soil and plant properties. The importance of spatial autocorrelations revealed in this study may be valuable for future research on soil carbon distribution and model improvement across spatial scales.

Acknowledgements

This work was supported by the Guangdong Flagship Project of Basic and Applied Basic Research (2023B0303050001), the National Natural Science Foundation of China (42177289 and U22A20449), the Spanish Government Grants PID2020115770RB-I, 2022-PID2022-141972NA-I00, and TED2021-132627B-I00 funded by MCIN, AEI/10.13039/501100011033 European Union NextGenerationEU/PRTR, the Catalan Government Grant SGR2021-1333, and the Fundación Ramón Areces Grant CIVP20A6621.

Data availability

All data that support the findings of this study are available from the corresponding author (Z.-F.L.) on request.

References

Adamczyk, B., Sietiö, O.M., Biasi, C., Heinonsalo, J., 2019. Interaction between tannins and fungal necromass stabilizes fungal residues in boreal forest soils. New Phytol. 223, 16-21.

Algora Gallardo, C., Baldrian, P., López-Mondéjar, R., 2021. Litter-inhabiting fungi show high level of specialization towards biopolymers composing plant and fungal biomass. Biol. Fertil. Soils 57, 77-88.

Al-Shammary, A. A. G., Kouzani, A. Z., Kaynak, A., Khoo, S. Y., Norton, M., & Gates, W., 2018. Soil bulk density estimation methods: A review. Pedosphere 28, 581-596.

Anselin, L., 1995. Local indicators of spatial association—LISA. Geog. Anal. 27, 93-115.

Bivand, R.S., Wong, D.W., 2018. Comparing implementations of global and local indicators of spatial association. Test 27, 716-748.

Bonan, G.B., 2008. Forests and climate change: forcings, feedbacks, and the climate benefits of forests. Science 320, 1444-1449.

Buckeridge, K.M., Creamer, C., Whitaker, J., 2022. Deconstructing the microbial necromass continuum to inform soil carbon sequestration. Funct. Ecol. 36, 1396-1410.

Buckeridge, K.M., Mason, K.E., McNamara, N.P., Ostle, N., Puissant, J., Goodall, T., Griffiths, R.I., Stott, A.W., Whitaker, J., 2020. Environmental and microbial controls on microbial necromass recycling, an important precursor for soil carbon stabilization. Commun. Earth Environ. 1, 36.

Burrough, P.A., McDonnell, R.A., Lloyd, C.D., 2015. Principles of geographical information systems, Oxford university press. Oxford.

Chen, G., Ma, S., Tian, D., Xiao, W., Jiang, L., Xing, A., Zou, A., Zhou, L., Shen, H., Zheng, C., Ji, C., He, H., Zhu, B., Liu, L., Fang, J., 2020. Patterns and determinants of soil microbial residues from tropical to

boreal forests. Soil Biol. Biochem. 151, 108059.

Cotrufo, M.F., Wallenstein, M.D., Boot, C.M., Denef, K., Paul, E., 2013. The Microbial Efficiency-Matrix Stabilization (MEMS) framework integrates plant litter decomposition with soil organic matter stabilization: do labile plant inputs form stable soil organic matter? Glob. Chang. Biol. 19, 988-995.

Dale, M. R., Fortin, M. J., 2014. Spatial analysis: a guide for ecologists. Cambridge University Press. Cambridge.

Elhorst, J.P., 2012. Dynamic spatial panels: models, methods, and inferences. J. Geogr. Syst. 14, 5-28.

Eswaran, H., Van Den Berg, E., Reich, P., 1993. Organic carbon in soils of the world. Soil Sci. Soc. Am. J. 57, 192-194.

Fan, X., Gao, D., Zhao, C., Wang, C., Qu, Y., Zhang, J., Bai, E., 2021. Improved model simulation of soil carbon cycling by representing the microbially derived organic carbon pool. ISME J. 15, 2248-2263.

Grosso, F., Bååth, E., De Nicola, F., 2016. Bacterial and fungal growth on different plant litter in Mediterranean soils: Effects of C/N ratio and soil pH. Appl. Soil Ecol. 108, 1-7.

He, L., Mazza Rodrigues, J.L., Soudzilovskaia, N.A., Barceló, M., Olsson, P.A., Song, C., Tedersoo, L., Yuan, F., Yuan, F., Lipson, D.A., Xu, X., 2020. Global biogeography of fungal and bacterial biomass carbon in topsoil. Soil Biol. Biochem. 151, 108024.

He, M., Fang, K., Chen, L., Feng, X., Qin, S., Kou, D., He, H., Liang, C., Yang, Y., 2022. Depth-dependent drivers of soil microbial necromass carbon across Tibetan alpine grasslands. Glob. Chang. Biol. 28, 936-949.

Hu, J., Huang, C., Zhou, S., Liu, X., Dijkstra, F.A., 2022. Nitrogen addition increases microbial necromass in croplands and bacterial necromass in forests: A global meta-analysis. Soil Biol. Biochem. 165, 108500.

Hu, Y., Zheng, Q., Noll, L., Zhang, S., Wanek, W., 2020. Direct measurement of the in situ decomposition of microbial-derived soil organic matter. Soil Biol. Biochem. 141, 107660.

Indorf, C., Dyckmans, J., Khan, K.S., Joergensen, R.G., 2011. Optimisation of amino sugar quantification by HPLC in soil and plant hydrolysates. Biol. Fertil. Soils 47, 387-396.

Joergensen, R.G., 2018. Amino sugars as specific indices for fungal and bacterial residues in soil. Biol. Fertil. Soils 54, 559-568.

Jones, D.L., Cooledge, E.C., Hoyle, F.C., Griffiths, R.I., Murphy, D.V., 2019. pH and exchangeable aluminum are major regulators of microbial energy flow and carbon use efficiency in soil microbial communities. Soil Biol. Biochem. 138, 107584.

Kärnä, O.-M., Heino, J., Laamanen, T., Jyrkänkallio-Mikkola, J., Pajunen, V., Soininen, J., Tolonen, K.T., Tukiainen, H., Hjort, J., 2019. Does catchment geodiversity foster stream biodiversity? Landscape Ecol. 34, 2469-2485.

Khan, K.S., Mack, R., Castillo, X., Kaiser, M., Joergensen, R.G., 2016. Microbial biomass, fungal and bacterial residues, and their relationships to the soil organic matter C/N/P/S ratios. Geoderma 271, 115-123.

Kimble, J.M., Follett, R.F., Stewart, B.A., 2000. Assessment methods for soil carbon, CRC press. Florida.

Kögel-Knabner, I., Rumpel, C., 2018. Advances in Molecular Approaches for Understanding Soil Organic Matter Composition, Origin, and Turnover: A Historical Overview. Adv. Agron. 149, 1-48.

Kuzyakov, Y., Bogomolova, I., Glaser, B., 2014. Biochar stability in soil: Decomposition during eight years and transformation as assessed by compound-specific 14C analysis. Soil Biol. Biochem. 70, 229-236.

Lefcheck, J.S., 2016. piecewiseSEM: Piecewise structural equation modelling in r for ecology, evolution, and systematics. Methods Ecol. Evol. 7, 573-579.

Lehmann, J., Kleber, M., 2015. The contentious nature of soil organic matter. Nature 528, 60-68.

Liang, C., Amelung, W., Lehmann, J., Kästner, M., 2019. Quantitative assessment of microbial necromass contribution to soil organic matter. Glob. Chang. Biol. 25, 3578-3590.

Liang, C., Cheng, G., Wixon, D.L., Balser, T.C., 2011. An Absorbing Markov Chain approach to understanding the microbial role in soil carbon stabilization. Biogeochemistry 106, 303-309.

Liang, C., Schimel, J.P., Jastrow, J.D., 2017. The importance of anabolism in microbial control over soil carbon storage. Nat. Microbiol. 2, 17105.

Locey, K.J., Muscarella, M.E., Larsen, M.L., Bray, S.R., Jones, S.E., Lennon, J.T., 2020. Dormancy dampens the microbial distance–decay relationship. PHILOS. T. R. SOC. B 375, 20190243.

Meyer, K.M., Memiaghe, H., Korte, L., Kenfack, D., Alonso, A., Bohannan, B.J.M., 2018. Why do microbes exhibit weak biogeographic patterns? ISME J. 12, 1404-1413.

Miltner, A., Bombach, P., Schmidt-Brücken, B., Kästner, M., 2012. SOM genesis: microbial biomass as a significant source. Biogeochemistry 111, 41-55.

Mori, T., Lu, X., Aoyagi, R., Mo, J., 2018. Reconsidering the phosphorus limitation of soil microbial activity in tropical forests. Funct. Ecol. 32, 1145-1154.

Mou, Z., Kuang, L., He, L., Zhang, J., Zhang, X., Hui, D., Li, Y., Wu, W., Mei, Q., He, X., Kuang, Y., Wang, J., Wang, Y., Lambers, H., Sardans, J., Peñuelas, J., Liu, Z., 2021. Climatic and edaphic controls over the

462 elevational pattern of microbial necromass in subtropical forests. Catena 207, 105707.
463 Müller, K., Marhan, S., Kandeler, E., Poll, C., 2017. Carbon flow from litter through soil microorganisms:
464 From incorporation rates to mean residence times in bacteria and fungi. Soil Biol. Biochem. 115, 187-
465 196.
466 Ni, X., Liao, S., Tan, S., Peng, Y., Wang, D., Yue, K., Wu, F., Yang, Y., 2020. The vertical distribution and
467 control of microbial necromass carbon in forest soils. Global Ecol. Biogeogr. 29, 1829-1839.
468 Pan, Y., Birdsey, R.A., Fang, J., Houghton, R., Kauppi, P.E., Kurz, W.A., Phillips, O.L., Shvidenko, A.,
469 Lewis, S.L., Canadell, J.G., Ciais, P., Jackson, R.B., Pacala, S.W., McGuire, A.D., Piao, S., Rautiainen,
470 A., Sitch, S., Hayes, D., 2011. A Large and Persistent Carbon Sink in the World's Forests. Science 333,
471 988-993.
472 Peng, W., Zhu, Y., Song, M., Du, H., Song, T., Zeng, F., Zhang, F., Wang, K., Luo, Y., Lan, X., Zhang, J.,
473 2019. The spatial distribution and drivers of soil microbial richness and diversity in a karst broadleaf
474 forest. For. Ecol. Manage. 449, 117241.
475 Prommer, J., Walker, T.W.N., Wanek, W., Braun, J., Zezula, D., Hu, Y., Hofhansl, F., Richter, A., 2020.
476 Increased microbial growth, biomass, and turnover drive soil organic carbon accumulation at higher plant
477 diversity. Glob. Chang. Biol. 26, 669-681.
478 R Core Team, 2021. Version 4.1.2. R: A language and environment for statistical computing. R Foundation
479 for Statistical Computing, Vienna, Austria. https://www.r-project.org.
480 Sayer, E.J., Heard, M.S., Grant, H.K., Marthews, T.R., Tanner, E.V.J., 2011. Soil carbon release enhanced
481 by increased tropical forest litterfall. Nat. Clim. Change 1, 304-307.
482 Sayer, E.J., Lopez-Sangil, L., Crawford, J.A., Bréchet, L.M., Birkett, A.J., Baxendale, C., Castro, B.,
483 Rodtassana, C., Garnett, M.H., Weiss, L., Schmidt, M.W.I., 2019. Tropical forest soil carbon stocks do
484 not increase despite 15 years of doubled litter inputs. Sci. Rep. 9, 18030.
485 Shao, P., Lynch, L., Xie, H., Bao, X., Liang, C., 2021. Tradeoffs among microbial life history strategies
486 influence the fate of microbial residues in subtropical forest soils. Soil Biol. Biochem. 153, 108112.
487 Song, M., Peng, W., Zeng, F., Du, H., Peng, Q., Xu, Q., Chen, L., Zhang, F., 2018. Spatial Patterns and
488 Drivers of Microbial Taxa in a Karst Broadleaf Forest. Front. Microbiol. 9, 1691.
489 Tang, X., Xia, M., Pérez-Cruzado, C., Guan, F., Fan, S., 2017. Spatial distribution of soil organic carbon
490 stock in Moso bamboo forests in subtropical China. Sci. Rep. 7, 1-13.
491 Tian, P., Zhao, X., Liu, S., Wang, Q., Zhang, W., Guo, P., Razavi, B.S., Liang, C., Wang, Q., 2022.

Differential responses of fungal and bacterial necromass accumulation in soil to nitrogen deposition in relation to deposition rate. Sci. Total Environ. 847, 157645.

Vasques, G.M., Grunwald, S., Comerford, N.B., Sickman, J.O., 2010. Regional modelling of soil carbon at multiple depths within a subtropical watershed. Geoderma 156, 326-336.

Wang, B., An, S., Liang, C., Liu, Y., Kuzyakov, Y., 2021. Microbial necromass as the source of soil organic carbon in global ecosystems. Soil Biol. Biochem. 162, 108422.

Wang, C., Qu, L., Yang, L., Liu, D., Morrissey, E., Miao, R., Liu, Z., Wang, Q., Fang, Y., Bai, E., 2021. Large-scale importance of microbial carbon use efficiency and necromass to soil organic carbon. Glob. Chang. Biol. 27, 2039-2048.

Wartenberg, D., 1985. Multivariate spatial correlation: a method for exploratory geographical analysis. Geog. Anal. 17, 263-283.

Whalen, E.D., Grandy, A.S., Sokol, N.W., Keiluweit, M., Ernakovich, J., Smith, R.G., Frey, S.D., 2022. Clarifying the evidence for microbial- and plant-derived soil organic matter, and the path toward a more quantitative understanding. Glob. Chang. Biol. 28, 7167-7185.

Wiesmeier, M., Urbanski, L., Hobley, E., Lang, B., von Lützow, M., Marin-Spiotta, E., van Wesemael, B., Rabot, E., Ließ, M., Garcia-Franco, N., Wollschläger, U., Vogel, H.-J., Kögel-Knabner, I., 2019. Soil organic carbon storage as a key function of soils - A review of drivers and indicators at various scales. Geoderma 333, 149-162.

Xia, Y., Chen, X., Zheng, X., Deng, S., Hu, Y., Zheng, S., He, X., Wu, J., kuzyakov, Y., Su, Y., 2020. Preferential uptake of hydrophilic and hydrophobic compounds by bacteria and fungi in upland and paddy soils. Soil Biol. Biochem. 148, 107879.

Xu, H., Li, Y., Lin, M., Wu, J., Luo, T., Zhou, Z., Chen, D., Yang, H., Liu, S., 2015. Community characteristics of a 60 ha dynamics plot in the tropical montane rain forest in Jianfengling, Hainan Island. Biodiversity Science 23, 192.

Yang, Y., Dou, Y., Wang, B., Wang, Y., Liang, C., An, S., Soromotin, A., Kuzyakov, Y., 2022. Increasing contribution of microbial residues to soil organic carbon in grassland restoration chronosequence. Soil Biol. Biochem. 170, 108688.

Yang, Y., Fang, J., Tang, Y., Ji, C., Zheng, C., He, J., Zhu, B., 2008. Storage, patterns and controls of soil organic carbon in the Tibetan grasslands. Glob. Chang. Biol. 14, 1592-1599.

Zhang, W., Cui, Y., Lu, X., Bai, E., He, H., Xie, H., Liang, C., Zhang, X., 2016. High nitrogen deposition

522 decreases the contribution of fungal residues to soil carbon pools in a tropical forest ecosystem. Soil Biol.
523 Biochem. 97, 211-214.
524 Zhao, X., Wang, Q., Kakubari, Y., 2009. Stand-scale spatial patterns of soil microbial biomass in natural
525 cold-temperate beech forests along an elevation gradient. Soil Biol. Biochem. 41, 1466-1474.

Figure captions

Fig. 1. The (A) location and (B) topographic map of Jianfengling 60-ha tropical montane rainforest. Red colour represents higher elevations, and blue colour indicates lower elevations.

Fig. 2: Summary of (A) soil microbial necromass carbon concentrations and (B) their proportions in SOC. MNC, microbial necromass carbon; FMNC, fungal-derived microbial necromass carbon; BMNC, bacterial-derived microbial necromass carbon; SOC, soil organic carbon (n = 500). SD, standard deviation; CV, coefficient of variations; P, *p* value of Kolmogorov-Smirnov test. Lowercase letters indicate significant difference between groups ($P < 0.05$, based on Dunn's non-parametric all-pairs comparison test).

Fig. 3. Spatial distribution of (A-C) soil microbial necromass carbon concentrations and (D-F) their proportions in SOC. (A) MNC, microbial necromass carbon; (B) FMNC, fungal-derived microbial necromass carbon; (C) BMNC, bacterial-derived microbial necromass carbon; (D) MNC/SOC ratio; (E) FMNC/SOC ratio; (F) BMNC/SOC ratio. SOC, soil organic carbon. Values are scaled from 0 (dark blue) to 1 (dark red).

Fig. 4. Spatial distribution of various environmental factors. Soil properties includes (A) sand; (B) silt; (C) clay; (D) SBD, soil bulk density; (E) SMC, soil moisture content; (F) SOC, soil organic carbon; (G) TN, total nitrogen concentration; (H) TP, total phosphorus concentration; (I) AP, plant-available phosphorus concentration; (J) pH; (K) C:N ratio; (L) C:P ratio; and (M) N:P ratio. Plant properties includes (N) richness, (O) abundance, and (P) biomass. Topographic features include (Q) elevation, (R) slope, (S) aspect, and (T) convexity. Values are scaled from 0 (dark blue) to 1 (dark red).

Fig. 5. Local spatial association map of (A-C) soil microbial necromass carbon concentrations and (D-F) their proportions in SOC. (A) MNC, microbial necromass carbon; (B) FMNC, fungal-derived microbial necromass carbon; (C) BMNC, bacterial-derived microbial necromass carbon; (D) MNC/SOC; (E) FMNC/SOC; (F) BMNC/SOC. SOC, soil organic carbon. High values surrounded by high values at $P < 0.05$ (red); low values surrounded by high values (orange); high values surrounded by low values (green); low values surrounded by low values (blue). The global indicators of spatial association were all significant at $P < 0.05$.

Fig. 6. Schematic plot of structural equations model accounting for the direct and indirect effects of topographic features, and soil and plant properties on (A) soil microbial necromass carbon concentrations and (B) their proportions in SOC. MNC, microbial necromass carbon; FMNC, fungal-derived microbial necromass carbon; BMNC, bacterial-derived microbial necromass carbon; SOC, soil organic carbon. Black and red lines represent positive and negative effects, respectively; and dashed lines indicate the effect is not significantly at $P < 0.05$.

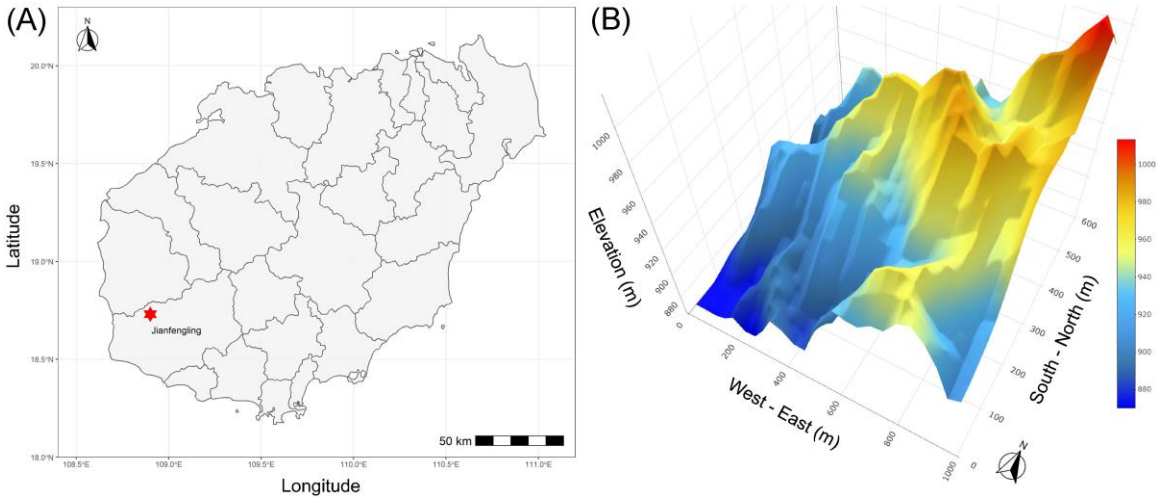

Figure 1

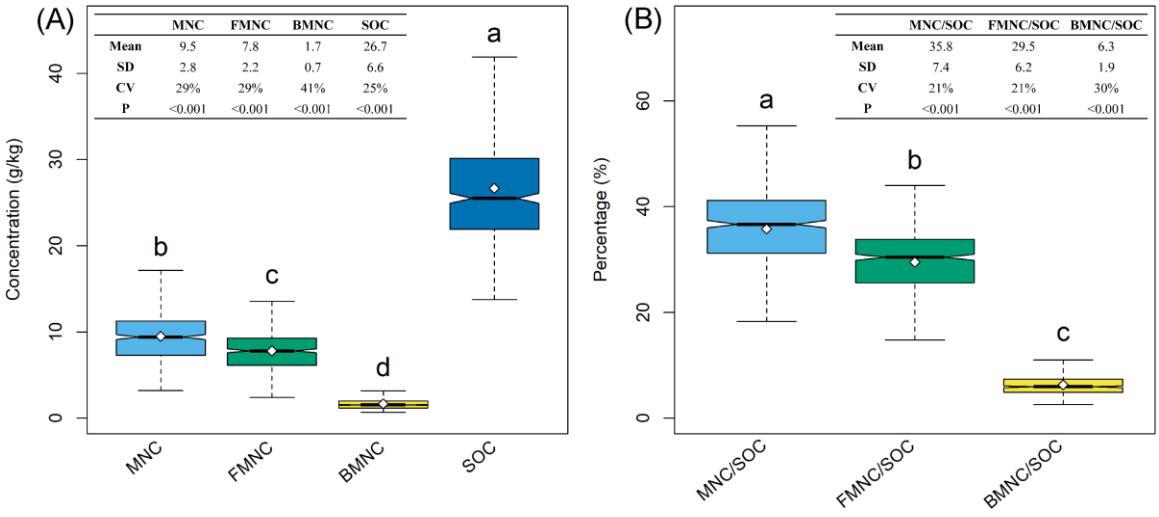

Figure 2

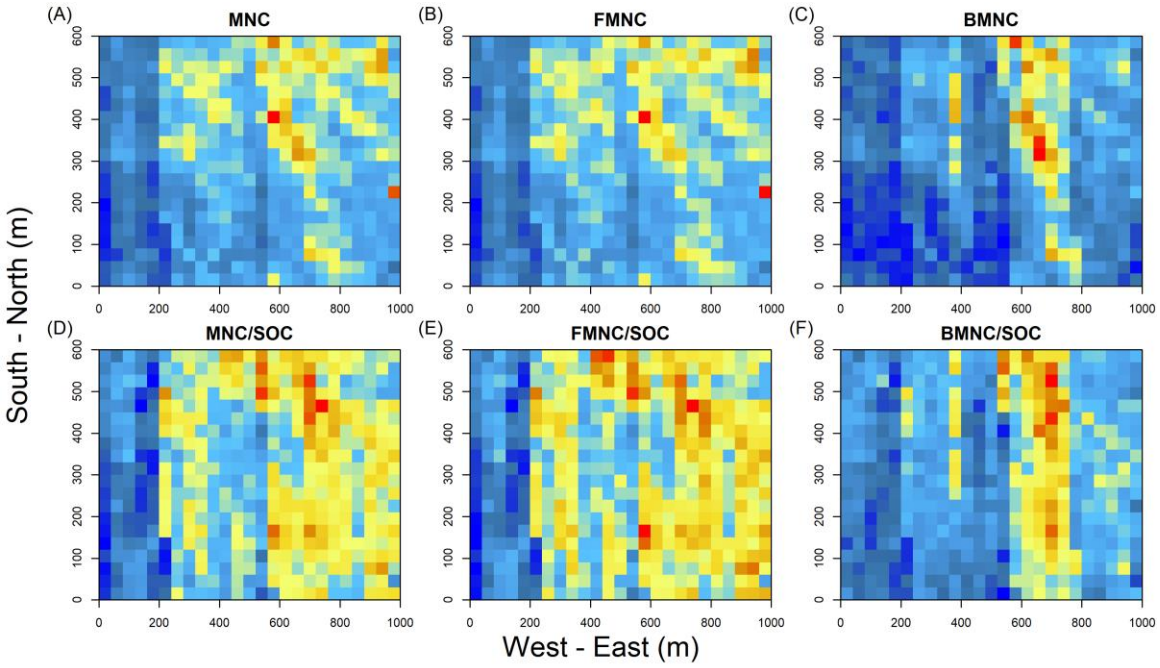

562

563 **Figure 3**

564

565

566

567

568

569

570

571

572

573

574

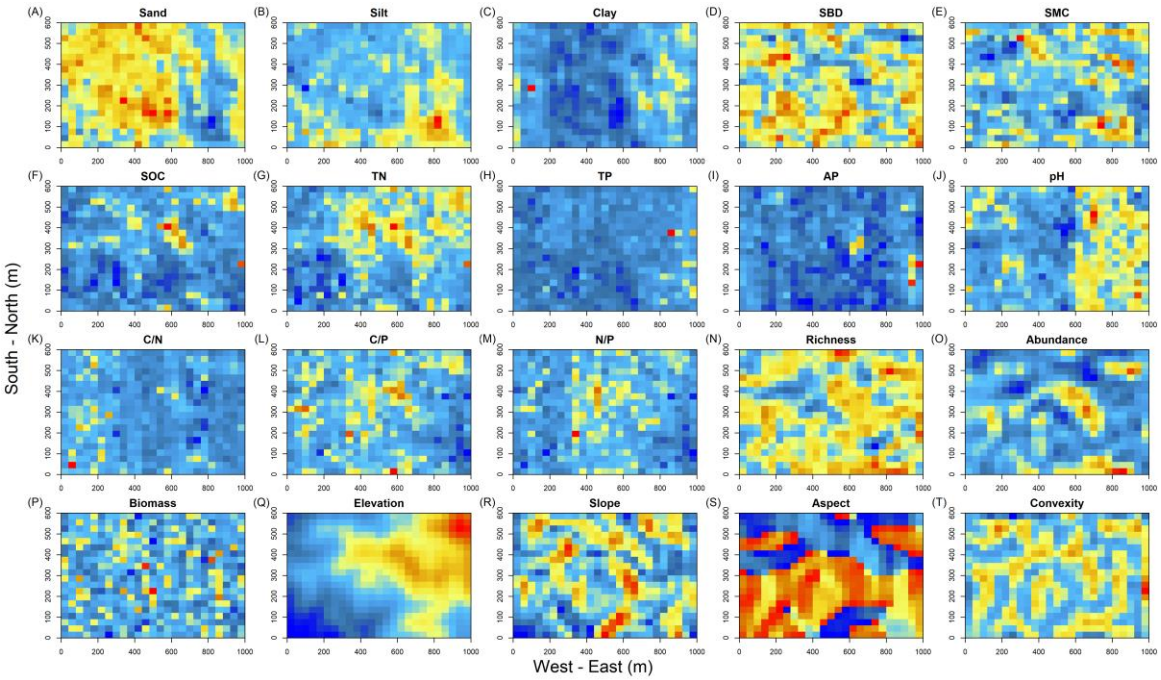

575

576 **Figure 4**

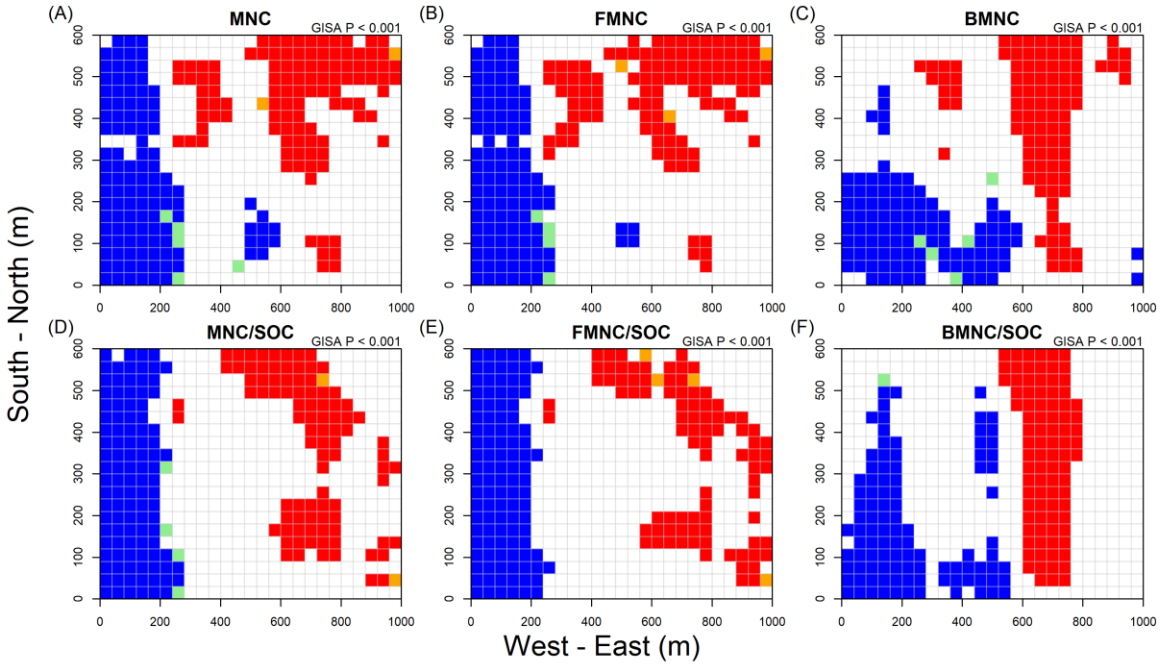

577

578 **Figure 5**

579

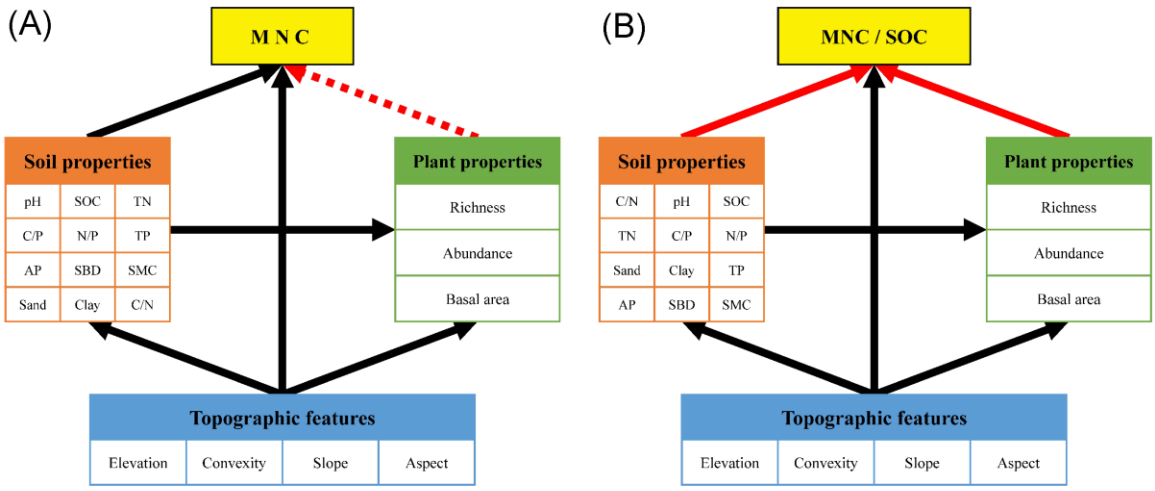

Total effects	MNC	FMNC	BMNC
Soil	0.675	0.695	0.445
Topographic	0.399	0.406	0.300
Plant	-	-	-

Total effects	MNC/SOC	FMNC/SOC	BMNC/SOC
Soil	-0.455	-0.471	-0.276
Topographic	-0.107	-0.114	-0.120
Plant	-0.079	-0.084	-

Figure 6